[Now published in full after the initial publication as an Epub ahead of print April 14, 2022 at www.fluorideresearch.online/epub/files/186.pdf]

FIRST PRINCIPLE STUDY OF STRUCTURAL, ELECTRONIC, ELASTIC AND OPTICAL PROPERTIES OF $TlXF_3$ (X = AG AND PD) EMPLOYING ACCURATE TB-MBJ APPROACH

Muhammad Tahir,[a] Mudasser Husain,[b] Nasir Rahman,[b,*] Mohammad Sohaibl,[b] Rajwali Khan,[b] Riadh Neffati,[c,d] Ghulam Murtaza,[e] Abid Ali Khan,[f] Anwar Iqbal,[f] Asad Ullah,[g] Aurangzeb Khan,[a,h]

Mardan, Lakki Marwat, and Peshawar, Pakistan; Abha, Saudi Arabia; and Tunis, Tunisia

ABSTRACT: This research presents within the full potential linearized augmented plane wave (FP-LAPW) technique with the first-principles calculations to investigate the structural, electronic, elastic and optical properties of ternary cubic perovskites of the form $TlXF_3$ (X= Ag and Pd) compounds. All these calculation is done by WIEN2k code within the density functional theory (DFT). The modified Becke–Johnson potential (TB-mBJ) is used for the optical and electronic properties. TDOS and PDOS analysis shows that both $TlAgF_3$ and $TlPdF_3$ are structurally stable and the main contribution of the states in $TlAgF_3$ compound is due to the Tl (d-orbitals) atoms and that in $TlPdF_3$ compound, F (p-states) contributes the more. The electronic-band structure analysis shows the metallic properties having no band gaps. Optical properties are also discussed using dielectric function. Elastic calculation revealed that both compounds are anisotropic, brittle and ionic.

Keywords: Density Functional Theory, Electronic property, Density of state, Optical property, Band structure, Elastic property.

1. INTRODUCTION

Any material have a nearly cubic crystal structure is called a Perovskite. The general chemical formula for perquisite compounds is ABX_3, where 'A', 'B' shows ions of different sizes, and X is an ion (frequently oxide) or fluorides that bonds to both ions. The 'A' atoms are generally larger than the atoms 'B' due to coordination number. Coordination number of A is 12 while the coordination number of B is 6. We will investigate the optical and electronic properties of both compounds in order to know their best use. Perovskites are used in various fields due to their wide range of electrical, optical, insulating and semiconducting behavior. Perovskites are found in the inner part of earth. Perovskite is being acknowledged among different materials with broad application in science and technology. It is used in electronic equipment's, renewable energy resources, and defense system due to their high photoelectric properties. The electrical resistance of perovskites changes when they are placed in

[a]Department of Physics, Abdul Wali Khan University, Mardan, Pakistan.
[b]Department of Physics, University of Lakki Marwat, 28420, Lakki Marwat, Khyber Pukhtunkhwa, Pakistan.
[c]Department of Physics – Faculty of Science – King Khalid University, P.O. Box 9004, Abha, Saudi Arabia.
[d]Laboratoire de Physique de la Matiére Condensée, Département de Physique, Faculté des Sciences de Tunis, Université Tunis El Manar, Tunis, Tunisia.
[e]Materials Modeling Lab, Department of Physics, Islamia College, Peshawar, Peshawar, Pakistan.
[f]Department of Chemical Sciences, University of Lakki Marwat, 28420, Lakki Marwat, Khyber Pukhtunkhwa, Pakistan.
[g]Department of Mathematical Sciences, University of Lakki Marwat, 28420, Lakki Marwat, Khyber Pukhtunkhwa.
[h]University of Lakki Marwat, 28420, Lakki Marwat, Khyber Pukhtunkhwa.
For correspondence: Nasir Rahman, Department of Physics, University of Lakki Marwat, 28420, Lakki Marwat, Khyber Pukhtunkhwa, Pakistan. E-mail: nasir@ulm.edu.pk

[Now published in full after the initial publication as an Epub ahead of print April 14, 2022 at www.fluorideresearch.online/epub/files/186.pdf]

the magnetic field. Perovskites compounds have same crystal structure as those of minerals and ceramics. Perovskite was discovered by Gustav Rose and was given the name "perovskite" in recognition of the important research work of Lev Perovski. Calcium titanate ($CaTiO_3$) is the chemical formula for natural occurring perovskite mineral [1]. Because of low refractive index, this fluoride-type material can be used for defense system, anti-reflection coating and in optics. The theoretical analysis of the structural and electronic properties of fluoride type prerequisites $TlAgF_3$ and $TlPdF_3$ are calculated. The modified Becke–Johnson potential (TB-mBJ) and exchange correlation is used within WIEN2k code [2] for application.

2. COMPUTATIONAL AND STRUCTURAL AND DETAIL

The structures for both the cubic fluoro Perovskites $TlAgF_3$ and $TlPdF_3$ having space group Pm-3m (#221) are shown in Figure 1. $TlAgF_3$ unit cell is occupied with Wyckoff positions: Tl = (0,0,0), Ag = (1/2, 1/2, 1/2) and F = (0, 1/2, 1/2). Similarly, for $TlPdF_3$ the occupied Wyckoff positions are Tl = (0 0 0), Pd = (1/2,1/2 1/2) and F = (0, 1/2,1/2). The number of k-points used in the Brillouin zone are 1,000. The potential wave and charge density are explained in the form of Fourier series vectors up to Gmax =12 au^{-1} [3].

In both structures, Tl, Ag and Pd change their sites. Lattice constant a = 4.52Å have been used for computation. The full potential linearized augmented plane wave (FP-LAPW) method of Kohn and Sham-density functional theory, is introduced in "WIEN2K code" to investigate the electronic structures [4]. The cut-off factor is:

$$R_{MT} \times K_{max} = 7$$

in which K_{max} shows the highest value of reciprocal lattice vector in the plane wave expansion, "R_{MT}" shows the lowest atomic sphere radius. The standard total energy calculation for the convergence of the self-consistent in density functional theory is 0.0001 Ry.

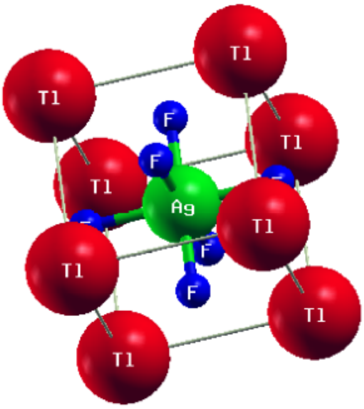

Figure 1. Crystal structure of $TlXF_3$ perovskite (X= Ag and Pd).

3. RESULTS AND DISCUSSIONS

3.1 VOLUME OPTIMIZATION

The structural optimization of $TlAgF_3$ and $TlPdF_3$ is calculated through Murnaghan's equation of state [5] to get equilibrium lattice constants. Volume optimization is the relaxed structure with minimum energy. Experimental values of the lattice parameters are slightly less than the observed values as shown in Figures 2A and 2B. The structural optimization defines the obtained energy versus volume plot for $TlAgF_3$ and $TlPdF_3$ are given in the Table 1. The equilibrium lattice constants (a), bulk modulus "B" and its pressure derivatives (B') are shown in Figures 2A and 2B. As the volume decreases, the initial energy of the unit cell increases. The lowest energy state (E_0) is acquired at a certain points where the energies of the system is minimum. Thus it is concluded that both the compounds are structurally stable at this point. This minimum volume corresponding to lowest energy level is known as optimized volume or ground state. Once ground state energy level is obtained, the system once again becomes unstable by increasing the unit cell volume. These investigation revealed for the first time and well matched with the given values in (AFLOW) literature [6]. Bulk modulus (B_0) shows the stiffness of the materials, which is greater for $TlAgF_3$ as compared for $TlPdF_3$. Therefore the $TlAgF_3$ is more soft and ductile as compared to $TlPdF_3$. It is also investigated that the energy needed to form TlAgF3 structure is greater than that for $TlPdF_3$.
The strength of the materials represent by bulk modulus "B" while pressure derivatives (B') is necessary to know thermoplastic properties of a material [7].

Table 1 Structural parameters i.e pressure derivatives 'B′' lattice constants 'a_0', and its bulk modulus 'B_0' at zero pressure.

Compound	Lattice constants a "Å"	Bulk modulus B_0 in (GPa)	Pressure Derivatives " B.´ "	Ground states energies "E_0"	Ground state Volume (v_0)
TlAgF3	4.43	110.05	7.23	-51775.82	552.71
TlPdF3	4.43	74.2579	5.6592	-51271.30	557.6924

[Now published in full after the initial publication as an Epub ahead of print April 14, 2022 at www.fluorideresearch.online/epub/files/186.pdf]

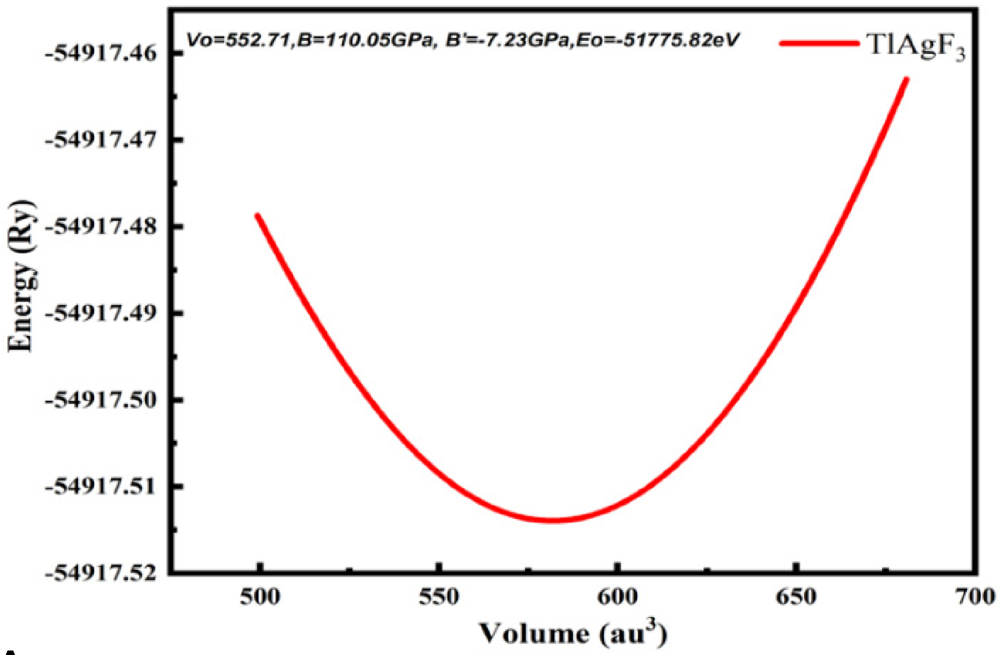

2A

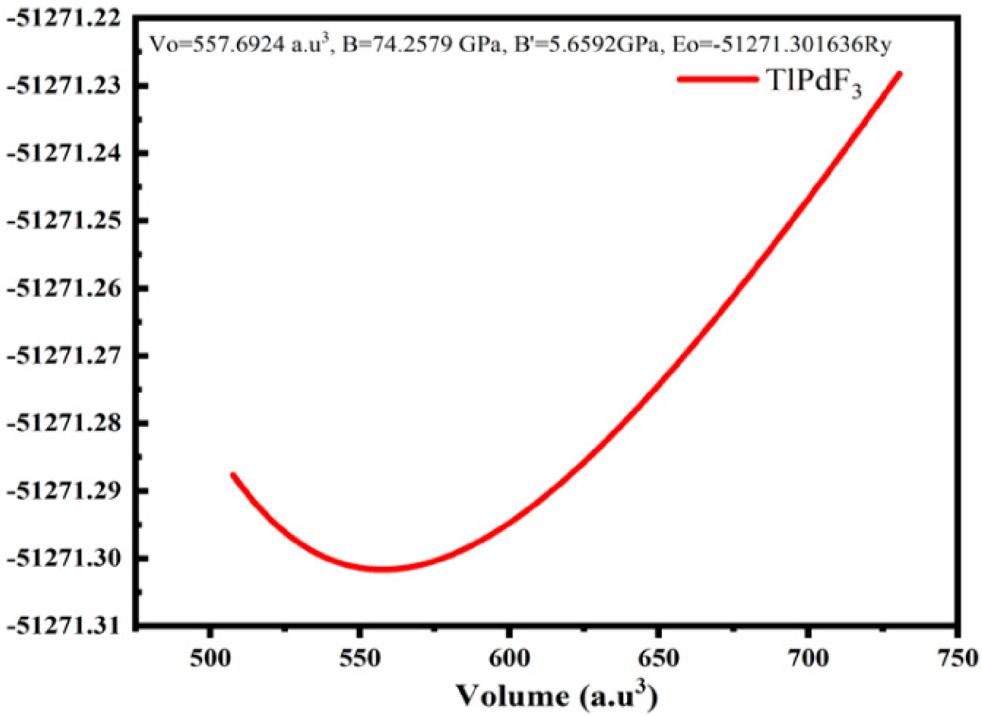

2B

Figures 2A and 2B. Volume optimization curves for $TlXF_3$ (X = Ag, Pd) cubic perovskites. 2A: $TlAgF_3$; 2B: $TlPdF_3$.

4. DENSITY OF STATES (DOS)

The density of states (DOS) illustrates the contributions of various electronic states and show an essential part to know the electronic properties of different materials. The total density of states (T-DOS) and partial density of states (P-DOS) of $TlAgF_3$ and $TlPdF_3$ compounds respectively are shown in Figures 3A and 3B.

The T-DOS plot of $TlAgF_3$ is shown in Figure 3A maximum peak in the valence band, are observed at -4.3 eV below the fermi level. Similarly two other small peaks of T-DOS plot are seen in the valence band due to F and Pd atoms at -4.3 eV and -2.1 eV respectively. In the P-DOS of $TlPdF_3$, the main contribution of F-p state electrons and less contribution of Tl-f state electrons in the conduction band above the fermi level. The total DOS peak lies at 7.0 eV and partial DOS are at 5.0 eV due to the contribution of Tl-p states electron respectively. However conduction and valence band overlaps and there is no band gap between. Hence $TlPdF_3$ are metallic in nature [8].

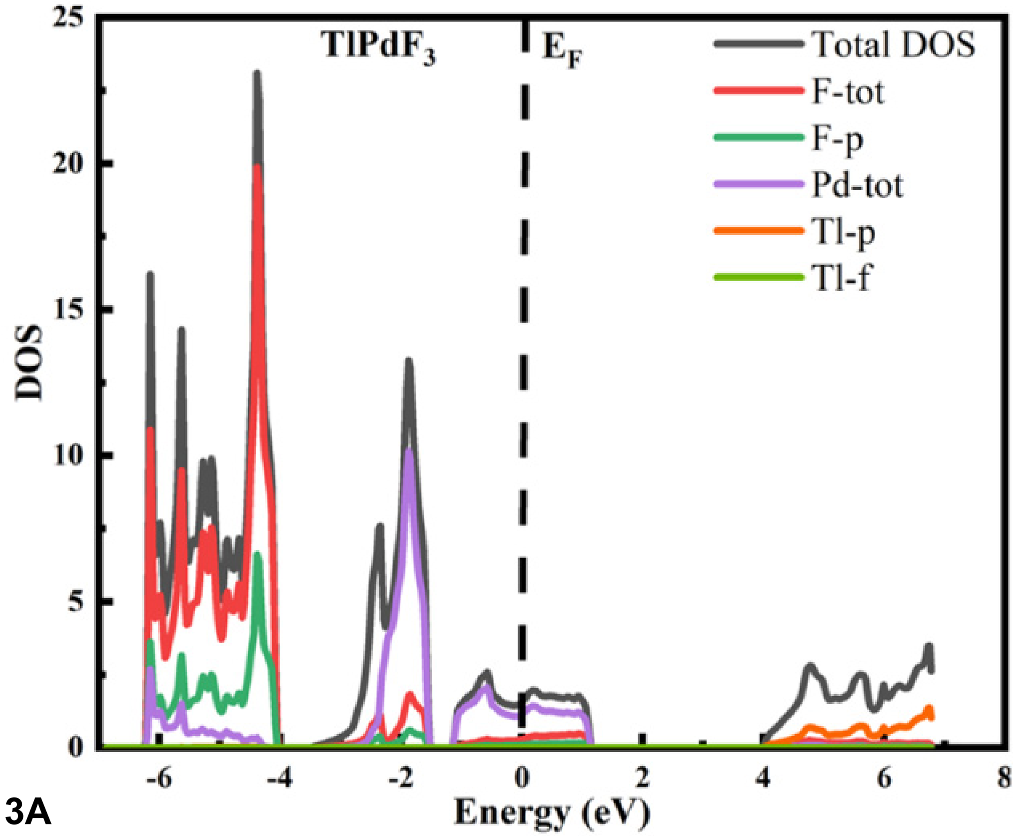

3A

Figure 3A: T-DOS and P-DOS of $TlPdF_3$.

[Now published in full after the initial publication as an Epub ahead of print April 14, 2022 at www.fluorideresearch.online/epub/files/186.pdf]

The total density of states (T-DOS) and partial density of states (P-DOS) plots of $TlAgF_3$ are shown in the Figure 3B. In the valence band, the total DOS peak of $TlAgF_3$ observed at -2.0 eV below the fermi level. In the case of partial density of states, the main contribution are due to Tl atoms individually which are in the valence region[9]. Two other small peaks are observed due to the contribution of p and d state electron in the valence region above the fermi level at -1.9 eV and -2.3 eV respectively. However there is no band gap between the valence and conduction band so $TlAgF_3$ are also metallic in nature[9].

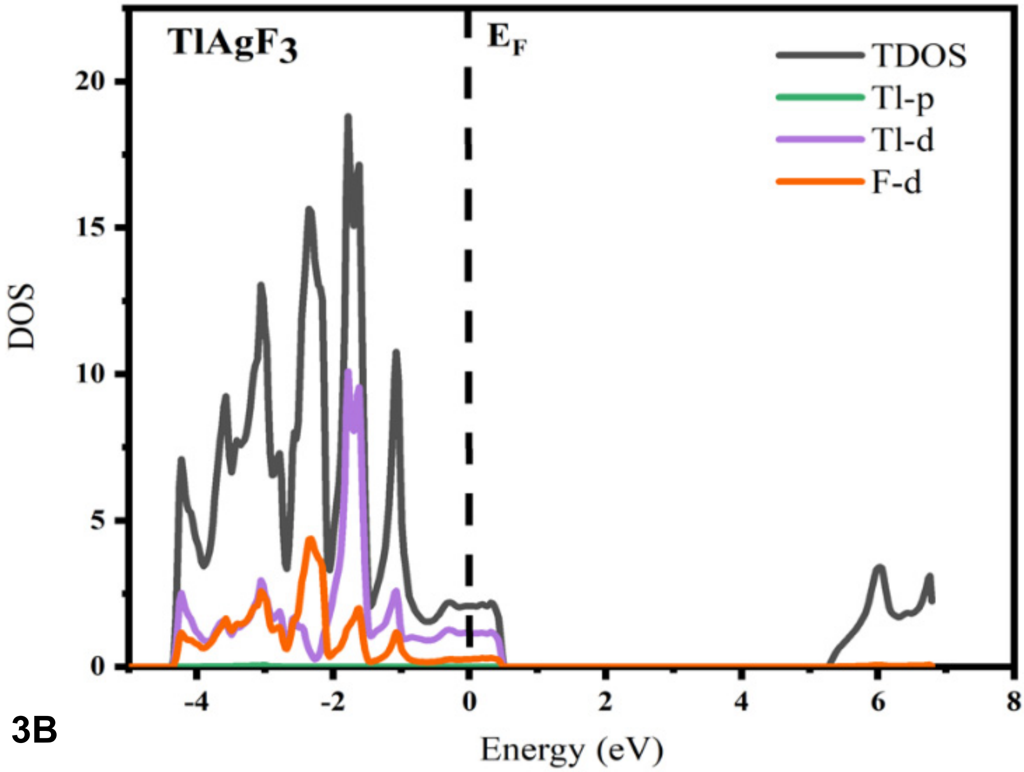

3B

Figure 3B. T-DOS and P-DOS of $TlAgF_3$.

5. Band Structures

The calculated electronic high-symmetry directions band structure for both fluoro-perovskites $TlAgF_3$ and $TlPdF_3$ of the Brillouin zone are illustrated in Figures 4A and 4B. Investigating the electronic band structure of these compounds can give us exact information of the best application in the fields of optics and electronics. Electronic band structure gives range of energy levels of electrons and also range of forbidden energy gaps. The electronic band structures were determined using the stable lattice constants.

As shown in Figures 4A and 4B. The electronic band structures of $TlAgF_3$ and $TlPdF_3$ on the selected "R-Γ-X-M-Γ"

[Now published in full after the initial publication as an Epub ahead of print April 14, 2022 at www.fluorideresearch.online/epub/files/186.pdf]

(TB-mBJ) method[10]. Fermi energy level is taken at 0.0 eV. Valence band maxima and conduction band minima lies on different symmetry points. The inner state electrons of Tl, Pd and F atoms in the Conduction band, the lowest energy band lies at 2.3 eV above Fermi level. At the symmetry point R in the valence region, the maximum band energy lies at 0.9 eV. In the conduction region, minimum energy occurs at 2.7 eV, at the symmetry point Γ above the Fermi level [10]. Thus it is concluded from the graph that along R - Γ symmetry directions, an indirect transition takes place. In this case our values are smaller than the band gap acquired from experiment al values (10.9 eV). The observed total DOS plot of $TlAgF_3$ is shown in Figure 4A.

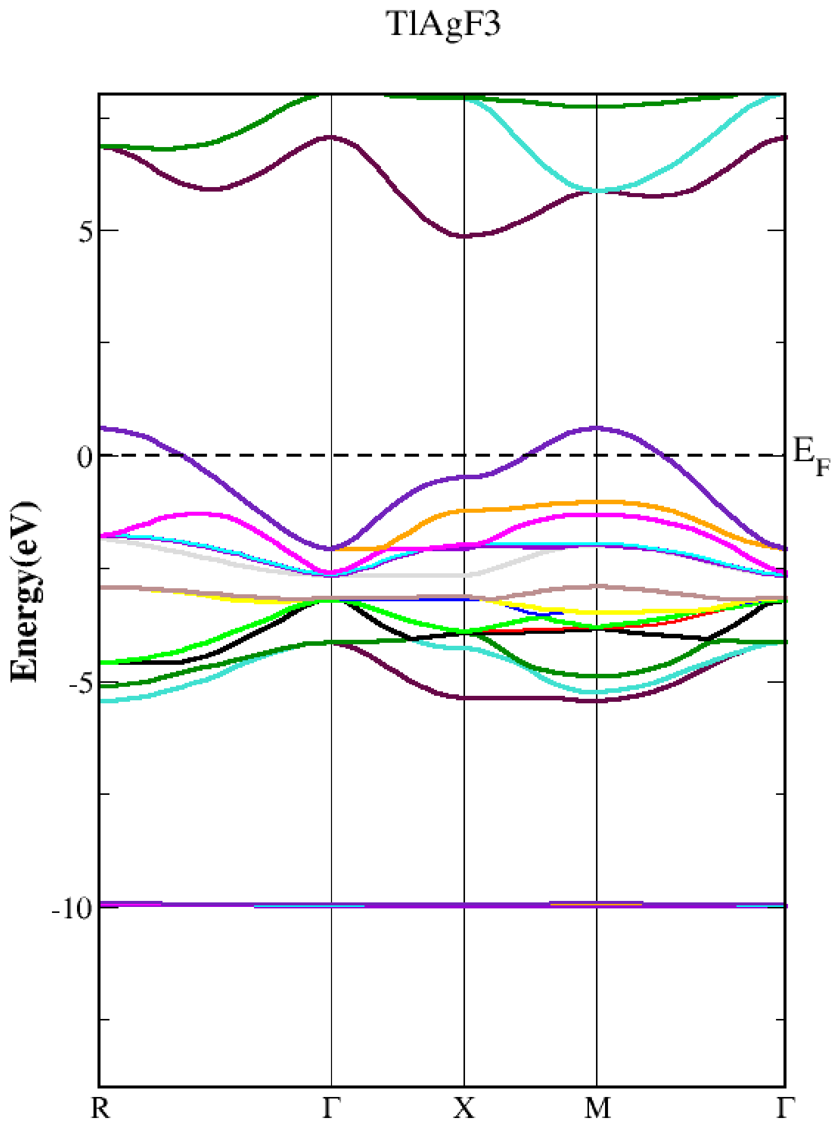

4A

Figure 4A. Shows band structures of $TlAgF_3$.

[Now published in full after the initial publication as an Epub ahead of print April 14, 2022 at www.fluorideresearch.online/epub/files/186.pdf]

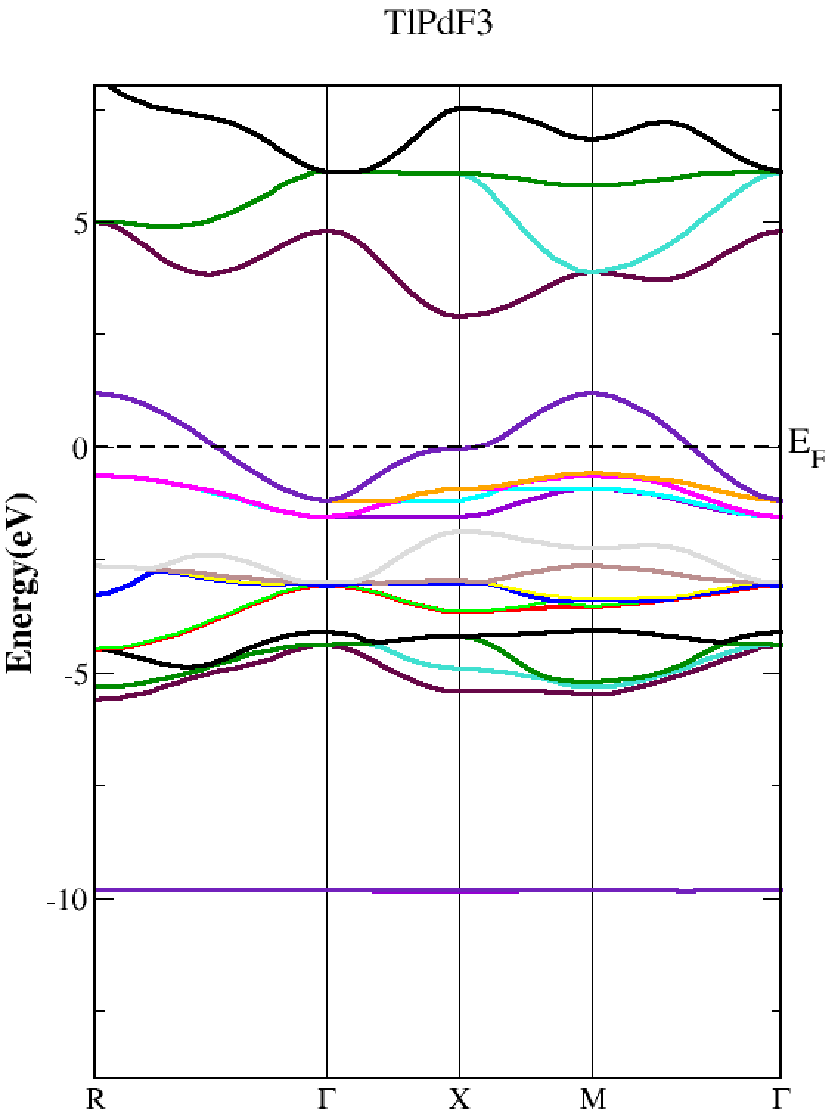

4B

Figure 4B. Shows band structures of $TlPdF_3$.

6. Optical properties

FP-LAPW method is used to determine the optical properties of both compounds. To analyze the result of $TlAgF_3$ and $TlPdF_3$ to incident photons, refractive index η(ω), Optical reflectivity R(ω), optical conductivity σ(ω), absorption coefficient **I**(ω), energy loss L(ω) and electron extinction coefficient K(ω)are determined [11]. The optical properties are described by means of the complex dielectric function

$$\varepsilon(\omega) = \varepsilon_1(\omega) + i\varepsilon_2(\omega) \qquad \text{(i)}$$

where $\varepsilon_1(\omega)$ and $\varepsilon_2(\omega)$ represents the real and imaginary parts respectively. The dielectric function and band structure of the electronic material are closely related to

[Now published in full after the initial publication as an Epub ahead of print April 14, 2022 at www.fluorideresearch.online/epub/files/186.pdf]

each other. The optical properties of material can be determined by dielectric function. The real component $\varepsilon_1(\omega)$ shows polarizability of a material. The calculated $\varepsilon_1(\omega)$ dielectric functions spectrum is shown in figure (x) and (y). The real part of the function "$\varepsilon_1(\omega)$" shows the electronic polarizability of a material [11]. The zero frequency limit $\varepsilon_1(0)$ is obtained at zero called static dielectric constant. This zero frequency limit lies nearly at as 5.2 in Figure 5 for $TlPdF_3$ and 4.3 for $TlAgF_3$. The electronic band structure and absorptive behavior of a material is described by $\varepsilon_2(\omega)$ of the dielectric function. It is the addition of all the transition between the valence band and the conduction band as shown by Figure 5. For imaginary part the threshold value of energy lying around 7.3 eV and 5.4 eV for $TlPdF_3$ and $TlAgF_3$.

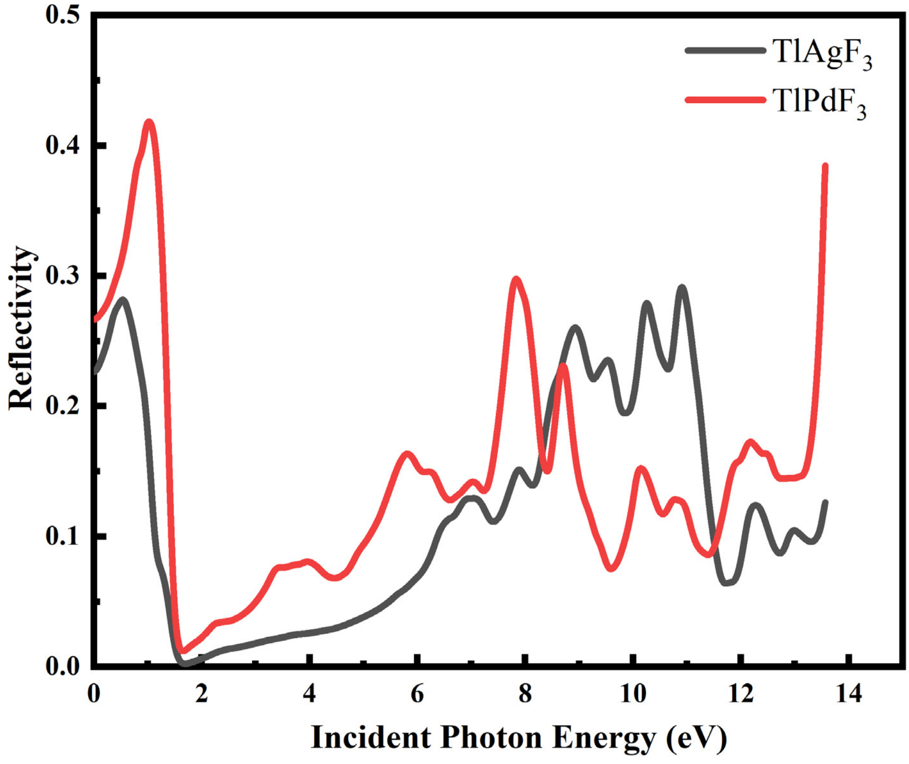

Figure 5. The calculated reflectivity R(ω) of $TlPdF_3$ and $TlAgF_3$.

6.1 THE REFLECTIVITY R(ω)

The reflectivity R(ω) spectrum is formed by sharing Tl-p states electrons in the valence band while X-d states electrons in the conduction band as seen in Figure 5 for $TlPdF_3$ and $TlAgF_3$. R(0) represents zero frequency reflectivity which is 10% for $TlPdF_3$ and 15% for $TlPdF_3$. The reflectivity coefficient "R(ω)" lies between 0.0 eV and 40eV and is smaller than 10% [12]. Reflectivity obtained at maximum value of 35% at 5.2eV for $TlPdF_3$ and 30% at 4.6eV for $TlAgF_3$ as shown in Figure 5.

6.2 The Refraction

Refractive index shows an important parameter and helpful in finding photoelectric effect [13]. So it is necessary to know all about the refraction of light. Optically isotropic nature of $TlPdF_3$ and $TlAgF_3$ are observed in the lower energies range. Refractive index represents complex number consists of real and imaginary numbers. Refractive index η(ω) are real parts of the function while K(ω) also known for extinction coefficient imaginary part as illustrated in Figure 6. For $TlPdF_3$ and $TlAgF_3$ the static refractive index η(0) lies at 2.8 and 3.3 respectively. For $TlPdF_3$, the highest refractive index rate is 5.0 at 3.9eV and 2.2eV for $TlAgF_3$.

Incident photon absorbed and slowed down by target material therefore their η(ω) value is greater than one [14]. Refractive index will be greater when a large number of photons slowed down due to interaction with a materials. Refractive index also depends on the type of bonding. Refractive index values in covalent bond is greater than ionic one because covalent bond share more electron than ionic [15]. Therefore due to covalent bonding maximum electrons are spread throughout the material and hence more chance for incident photon to be slowed down. The extinction coefficient K(ω) (imaginary part) are shown in Figure.6.

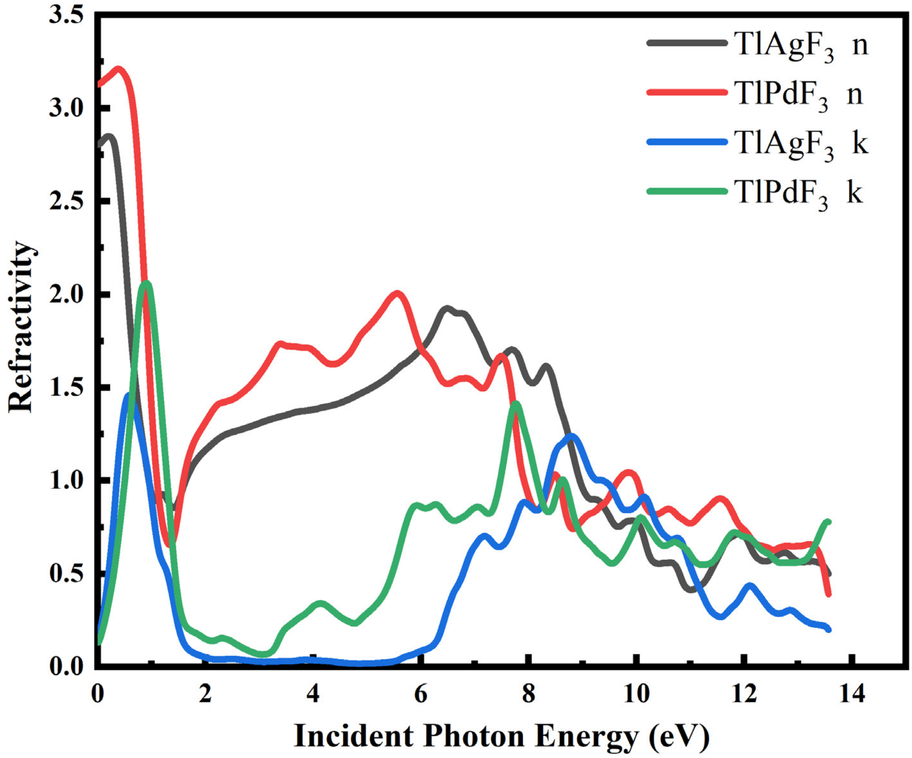

Figure 6. The refractive index η(ω) of $TlPdF_3$ and $TlAgF_3$.

6.3. THE CONDUCTIVITY σ(ω)

Optical conductivity σ(ω) is the electron conductivity due to applied electromagnetic field [16]. The calculated σ(ω) for $TlPdF_3$ and $TlAgF_3$ are shown in fig.7. The optical conductivity σ(ω) spectra increases sharply at a point called critical point of 35 eV for $TlPdF_3$ and at 7 eV for $TlAgF_3$. The highest optical conductivity σ(ω) recorded approximately to be 4300 $\Omega^{-1}cm^{-1}$ at 8 eV for $TlAgF_3$ and for $TlAgF_3$ it is 3900 $\Omega^{-1}cm^{-1}$ at 8.3 eV.

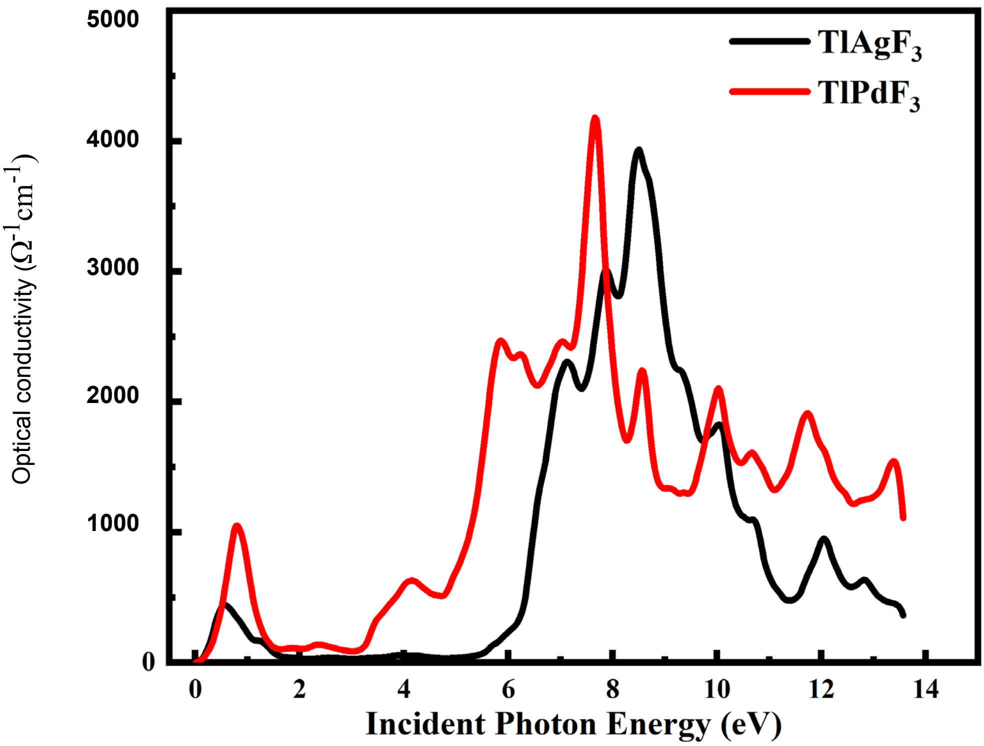

Figure 7. The conductivity σ(ω) of $TlPdF_3$ and $TlAgF_3$.

6.4 THE ABSORPTION I(ω)

Figure 8 shows the analysis of absorption coefficient I(ω) for both $TlPdF_3$ and $TlAgF_3$ compounds. Both compounds show proper absorption on incident radiation and then it starts absorbing electromagnetic radiation at certain point called threshold point [17]. Threshold points for $TlPdF_3$ is to be 1.6eV while for and $TlAgF_3$ it is 2.3eV respectively. In our case the maximum absorption is at 7.5eV and 8.9eV for $TlPdF_3$ and $TlAgF_3$ respectively.

.

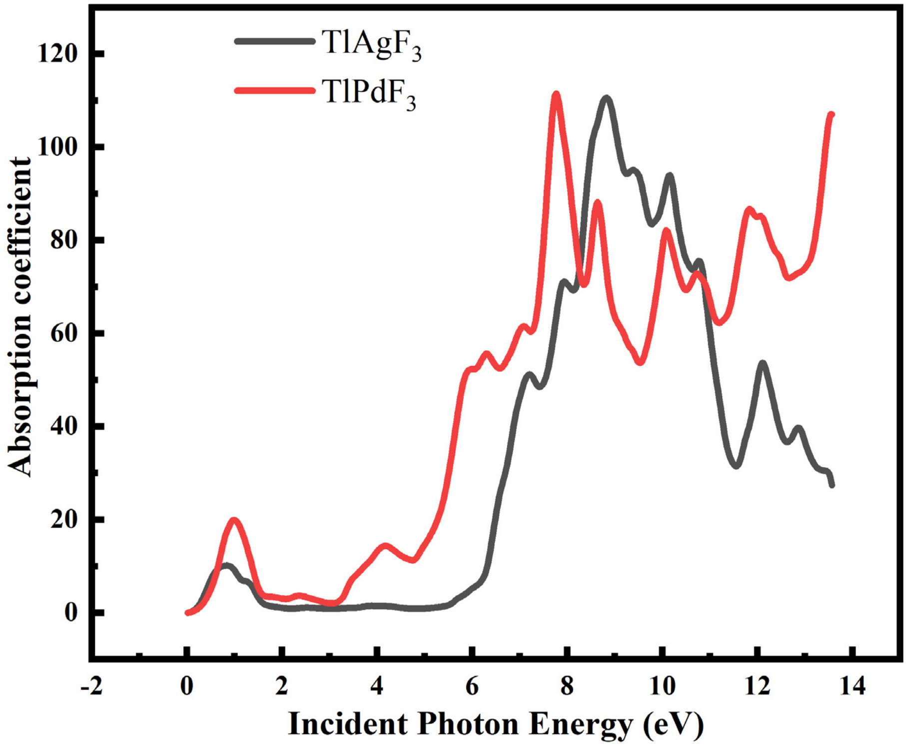

Figure 8. The calculated absorption coefficient I(ω) of $TlPdF_3$ and $TlAgF_3$.

7. Elastic properties

For simple cubic structure $C_{i,j}$ (where i = 1, 1, 4 and j = 1, 2, 4) are three independent elastic constants. The FP-LAPW scheme is used in wien2k package. The cubic unit cell is deformed to find out these constants using proper strain tensor to yield an energy–strain relation [18].

The elastic constants C_{ij} are calculated for the compounds $TlPdF_3$ and $TlAgF_3$. The computed elastic constants are summarized in Table 2. Mechanical properties can be analyzed by using these elastic constant C_{ij}. Bulk modulus 'B' are positive and therefore these constants are positive [19]. Elastic constants C_{ij} constant of solids provide information that how deformation produced and then retrieve to restore their position after the removal of stress. Certain information like an-isotropic behavior and the bonding character can be find out by C_{ij}. Charpin used WIEN2K package to find out these elastic parameters [20]. The calculated bulk modulus and elastic constants from the theoretical elastic constants are shown in Table 2.

$(C_{11}–C_{12})$ is greater than 0, $(C_{11}+2C_{121})$ is greater than 0 and C_{44} is also greater than 0. The mechanical stability in a cubic crystal is described by B: $C_{12} < B < C_{11}$.

The elastic parameters like A, G, E and *v* are used in the following relations[20].

[Now published in full after the initial publication as an Epub ahead of print April 14, 2022 at www.fluorideresearch.online/epub/files/186.pdf]

$$A = 2C_{44} / C\,11 - C\,12 \qquad \text{(ii)}$$

$$E = 9GB / 3B+G \qquad \text{(iii)}$$

$$v = 3B - 2G / 2\,(2B + G) \qquad \text{(iv}$$

$$G = ½\,(G_V + G_R)$$

$$G_V = ½\,(C11 - C12 + 3C44) \qquad \text{(v)}$$

$$G_R = 5C_{44}(C_{11}\text{-}C_{12}) / 4C_{44}+3(C_{11}\text{-}C_{12}) \qquad \text{(vi)}$$

Table. 2 The obtained Cij and other mechanical parameters

Compound	C_{11}	C_{12}	C_{44}	B	A	G	E	υ	B/G
$TlPdF_3$	220.50	76.00	28.03	110	0.388	90.5	212	0.24	1.22
$TlAgF_3$	176.0	50.7	20.5	74	0.31	74	296	0.20	1.00

"G" represents shear modulus, "G_V" gives Voigt's shear modulus with the upper limit of "G" values, "G_R" shows Reuss's shear modulus with subscript "G" values [21]. A is nearly equals to one for an-isotropic compounds, while deviation from A shows an-isotropy. The rate of anisotropy measures the value of variation from one. In our calculation, the rate of an-isotropy factor is 0.388 and 0.31 for $TlPdF_3$ and for $TlAgF_3$ respectively. Hence both materials are an-isotropic. Both materials are highly strong as E values for are very high. E values shows stiffness of the materiel, as it is a fine marking regarding the strength of the material. *v* is the Poisson's ratio, which is very low for covalent materials, i.e, less than 0.1 and nearly equal to 0.25 for ionic compounds. In our case, *v* is 0.24 for $TlPdF_3$ and 0.20 for $TlAgF_3$. Therefore $TlPdF_3$ and for $TlAgF_3$ are ionic in nature and should be assume an intrabonding.

Both these compounds didn't satisfy Pugh's criteria as indicated by the B/G relation. This relation shows the mechanical properties of material like brittleness and ductility [22]. $TlPdF_3$ and $TlAgF_3$ are brittle as both compounds didn't satisfy Pugh's criteria. If $B/G > 1.75$, then the material is said to be ductile and this value is the standard for material ductility. In our study, the B/G ratio for $TlPdF_3$ is 1.22 and 1.00 for $TlAgF_3$, and hence our compounds are brittle.

CONCLUSIONS

Herein, we investigated the electronic, structural, elastic and optical properties of fluoro-perovskites $TlAgF_3$ and $TlPdF_3$ using full potential linearized augmented plane wave method under generalized gradient approximations within Wien2k. From the volume optimization, the optimized lattice constants, bulk modulus (B), and its pressure derivatives of both cubic fluoro-perovskites are investigated. The total DOS plot of TlAgF3 and $TlPdF_3$ are examined. In $TlPdF_3$ compound, the maxima in peaks in the valence region are due to only F atom. This is also evident from the partial DOS plots of Tl, Pd, Ag, and F atoms respectively. We have found from our study that the band gap of $TlAgF_3$ and $TlPdF_3$ overlaps and hence $TlAgF_3$ and $TlPdF_3$ are metallic in nature. Measured the elastic constants (C_{ij}) and elastic module. It is investigated from the elastic properties computation that both compounds are highly stable and hard. Some optical properties like absorption, dielectric function and refractive index are calculated. Static dielectric constant ε_1 (o) are approximately 2.24 and the static refractive index η (o) is nearly 1.5.

.REFERENCES

[1] S. Arya *et al.* A comprehensive review on synthesis and applications of single crystal perovskite halides. *Prog. Solid State Chem.*, vol. 60, p. 100286, Dec. 2020, doi: 10.1016/J.PROGSOLIDSTCHEM.2020.100286.

[2] E. G. Özdemir and Z. Merdan. Half-metal calculations of CoZrGe half-Heusler compound by using generalized gradient approximation (GGA) and modified Becke-Johnson (mBJ) methods. *Mater. Res. Express*, vol. 6, no. 11, p. 116124, Nov. 2019, doi: 10.1088/2053-1591/AB502B.

[3] G. Rogl *et al.* High-ZT half-Heusler thermoelectrics, Ti0.5Zr0.5NiSn and Ti0.5Zr0.5NiSn0.98Sb0.02: Physical properties at low temperatures. *Acta Mater.*, vol. 166, pp. 466–483, Mar. 2019, doi: 10.1016/J.ACTAMAT.2018.12.042.

[4] S. Belhachi. Accurate Bandgap of Zr x Al1-x N Using Modified Becke–Johnson (mBJ) Exchange Potential. *J. Supercond. Nov. Magn. 2017 315*, vol. 31, no. 5, pp. 1545–1548, Sep. 2017, doi: 10.1007/S10948-017-4364-2.

[5] B. Wu, M. Zinkevich, F. Aldinger, D. Wen, and L. Chen. Ab initio study on structure and phase transition of A- and B-type rare-earth sesquioxides Ln2O3 (Ln=La–Lu, Y, and Sc) based on density function theory. *J. Solid State Chem.*, vol. 180, no. 11, pp. 3280–3287, Nov. 2007, doi: 10.1016/J.JSSC.2007.09.022.

[6] J. M. Hawkins, J. F. Weaver, and A. Asthagiri. Density functional theory study of the initial oxidation of the Pt(111) surface. *Phys. Rev. B - Condens. Matter Mater. Phys.*, vol. 79, no. 12, p. 125434, Mar. 2009, doi: 10.1103/PHYSREVB.79.125434/FIGURES/12/MEDIUM.

[7] I. Zeba, R. Kiran, M. Shakil, M. Rafique, R. Ahmad, and S. S. A. Gillani. Study the effect of magnesium doping concentration on structural and optoelectronic response of NaCa1-xMgxF3 fluoro-perovskite: First-principles computation. *Optik (Stuttg).*, vol. 218, p. 164990, Sep. 2020, doi: 10.1016/J.IJLEO.2020.164990.

[8] J. Saddique *et al.* Modeling structural, elastic, electronic and optical properties of ternary cubic barium based fluoroperovskites $MBaF_3$ (M = Ga and In) compounds based on DFT. *Mater. Sci. Semicond. Process.*, vol. 139, p. 106345, Mar. 2022, doi: 10.1016/J.MSSP.2021.106345.

[9] A. Abdullah *et al.* Computational investigation of structural, magnetic, elastic, and electronic properties of Half-Heusler ScVX (X = Si, Ge, Sn, and Pb) compounds. *Eur. Phys. J. Plus 2021 13611*, vol. 136, no. 11, pp. 1–9, Nov. 2021, doi: 10.1140/EPJP/S13360-021-02175-4.

[10] M. Husain *et al.* Structural, electronic, elastic, and magnetic properties of NaQF3 (Q=ag, Pb, Rh, and Ru) flouroperovskites: A first-principle outcomes. *Int. J. Energy Res.*, vol. 46, no. 3, pp. 2446–2453, Mar. 2022, doi: 10.1002/ER.7319.

[11] N. Rahman *et al.* First principle study of structural, electronic, optical and mechanical properties of cubic fluoro-perovskites: (CdXF3, X = Y, Bi). *Eur. Phys. J. Plus 2021 1363*, vol. 136, no. 3, pp. 1–11, Mar. 2021, doi: 10.1140/EPJP/S13360-021-01177-6.

[12] G. Murtaza and I. Ahmad. First principle study of the structural and optoelectronic properties of cubic perovskites $CsPbM_3$ (M=Cl, Br, I). *Phys. B Condens. Matter*, vol. 406, no. 17, pp. 3222–3229, Sep. 2011, doi: 10.1016/J.PHYSB.2011.05.028.

[13] R. Sabetvand, M. E. Ghazi, and M. Izadifard. Studying temperature effects on electronic and optical properties of cubic CH3NH3SnI3 perovskite. *J. Comput. Electron. 2020 191*, vol. 19, no. 1, pp. 70–79, Jan. 2020, doi: 10.1007/S10825-020-01443-3.

[14] T. H. Kim *et al.* Polar metals by geometric design. *Nat. 2016 5337601*, vol. 533, no. 7601, pp. 68–72, Apr. 2016, doi: 10.1038/nature17628.

[15] M. Shinagawa, J. Kobayashi, S. Yagi, and Y. Sakai. Sensitive electro-optic sensor using KTa1-xNbxO3 crystal,.*Sensors Actuators A Phys.*, vol. 192, pp. 42–48, Apr. 2013, doi: 10.1016/J.SNA.2012.12.003.

[16] D. B. Mitzi, K. Chondroudis, and C. R. Kagan. Design, structure, and optical properties of organic-inorganic perovskites containing an oligothiophene chromophore. *Inorg. Chem.*, vol. 38, no. 26, pp. 6246–6256, 1999, doi: 10.1021/IC991048K/SUPPL_FILE/IC991048K_S.PDF.

[17] R. Lu and A. M. Hofmeister. ìnfrared spectroscopy of CaGeO3 perovskite to 24 GPa and thermodynamic implications. *Phys. Chem. Miner. 1994 211*, vol. 21, no. 1, pp. 78–84, 1994, doi: 10.1007/BF00205218.

[18] J. M. Whitney and M. B. Riley. Elastic properties of fiber reinforced composite materials. Available from: https://doi.org/10.2514/3.3732, vol. 4, no. 9, pp. 1537–1542, May 2012, doi: 10.2514/3.3732.

[19] J. Qu. The effect of slightly weakened interfaces on the overall elastic properties of composite materials. *Mech. Mater.*, vol. 14, no. 4, pp. 269–281, Mar. 1993, doi: 10.1016/0167-6636(93)90082-3.

[20] J. G. Berryman. Theory of elastic properties of composite materials. *Appl. Phys. Lett.*, vol. 35, no. 11, p. 856, Aug. 2008, doi: 10.1063/1.90982.

[21] S. I. Rokhlin and W. Wang. Ultrasonic Evaluation of in-Plane and out-of-Plane Elastic Properties of Composite Materials. *Rev. Prog. Quant. Nondestruct. Eval.*, pp. 1489–1496, 1989, doi: 10.1007/978-1-4613-0817-1_187.

[22] R. RodrÌguez-Ramos, R. de Medeiros, R. Guinovart-DÌaz, J. Bravo-Castillero, J. A. Otero, and V. Tita, Different approaches for calculating the effective elastic properties in composite materials under imperfect contact adherence. *Compos. Struct.*, vol. 99, pp. 264–275, May 2013, doi: 10.1016/J.COMPSTRUCT.2012.11.040.